

Accepted Manuscript

Influence of upper rim dibromo-substitution in bis-1,3-diketone calix[4]arenes on spectral properties of ligands and their lanthanide complexes

Sergey N. Podyachev, Gulnaz Sh. Gimazetdinova, Svetlana N. Sudakova, Nataliya A. Shamsutdinova, Dmitry V. Lapaev, Victor V. Syakaev, Aidar T. Gubaidullin, Rinas N. Nagimov, Asiya R. Mustafina

PII: S0040-4020(17)30785-8

DOI: [10.1016/j.tet.2017.07.043](https://doi.org/10.1016/j.tet.2017.07.043)

Reference: TET 28875

To appear in: *Tetrahedron*

Received Date: 15 May 2017

Revised Date: 13 July 2017

Accepted Date: 24 July 2017

Please cite this article as: Podyachev SN, Gimazetdinova GS, Sudakova SN, Shamsutdinova NA, Lapaev DV, Syakaev VV, Gubaidullin AT, Nagimov RN, Mustafina AR, Influence of upper rim dibromo-substitution in bis-1,3-diketone calix[4]arenes on spectral properties of ligands and their lanthanide complexes, *Tetrahedron* (2017), doi: 10.1016/j.tet.2017.07.043.

This is a PDF file of an unedited manuscript that has been accepted for publication. As a service to our customers we are providing this early version of the manuscript. The manuscript will undergo copyediting, typesetting, and review of the resulting proof before it is published in its final form. Please note that during the production process errors may be discovered which could affect the content, and all legal disclaimers that apply to the journal pertain.



Influence of upper rim dibromo-substitution in bis-1,3-diketone calix[4]arenes on spectral properties of ligands and their lanthanide complexes

Sergey N. Podyachev ^{a*}, Gulnaz Sh. Gimazetdinova ^b, Svetlana N. Sudakova ^a, Nataliya A. Shamsutdinova ^a, Dmitry V. Lapaev ^c, Victor V. Syakaev ^a, Aidar T. Gubaidullin ^a, Rinas N. Nagimov ^b, Asiya R. Mustafina ^a

^a *A. E. Arbuzov Institute of Organic and Physical Chemistry, Kazan Scientific Center of Russian Academy of Sciences, Arbuzov str., 8, 420088, Kazan, Russia.*

^b *Kazan National Research Technological University, K. Marks str., 68, 420015, Kazan, Russia.*

^c *Zavoisky Physical-Technical Institute of Kazan Scientific Center of Russian Academy of Sciences, 420029 Kazan, Russia.*

Abstract: The present work introduces the synthesis and characterization of upper rim dibromo-substituted bis-1,3-diketone calix[4]arenes with hydroxy and propyloxy groups at the lower rim as ligands for Gd³⁺ and Tb³⁺ complexes. The dibromo-substitution does not affect 1:1 complex formation with the lanthanide ions arising from their coordination via two 1,3-diketonate groups incorporated at the upper rim of the calix[4]arene. The analysis of the time-resolved luminescence spectra of the Gd³⁺ complexes clearly demonstrates the notable enhancement of the decay time of the ligand triplet state, while the energy of the triplet state for the new dibromo-bis-1,3-diketones remains practically unchanged versus its non-substituted analogues. The latter tendency points to the heavy-atom effect on the energy transfer from the excited state to vibration levels of the dibromo-substituted ligand resulting in a decreased radiationless decay contribution. Measurements of Tb³⁺-centered luminescence indicate a better antenna effect (~1.7) of dibromo-calix[4]arenes compared with its non-substituted counterpart.

Keywords: calixarenes; ketones; luminescence; chelates; lanthanides

* Corresponding author. *A. E. Arbuzov Institute of Organic and Physical Chemistry, Kazan Scientific Center of Russian Academy of Sciences, Arbuzov str., 8, 420088, Kazan, Russia.*

E-mail: spodyachev@iopc.ru

<http://dx.doi.org/XXXXXXXXXXXXXX>.

1. Introduction

The unique photophysical properties of lanthanide complexes make them promising building blocks in the development of advanced luminescent materials for bio-medical diagnostics,¹⁻³ optoelectronics,⁴ OLED's and solar energy conversion.⁵⁻⁷ The forbidden nature of 4f-4f electronic transitions results in a low absorption of UV-visible light by lanthanide ions. Thus, the population of an excited state of lanthanide ion ligand-to-metal energy transfer is of great impact in a lanthanide-centered luminescence efficacy.⁸ This in turn emphasizes the importance of ligand's spectral properties and complex formation ability in their antenna-effect on lanthanide-centered luminescence.⁹⁻¹³

The substituent's effect is a well-known tool in the design of both complexing ability and photophysical properties of ligands.¹⁴⁻¹⁶ The calix[4]arene backbone provides a convenient basis for embedding various substituents in order to guide the properties of the ligand. Our previous reports highlight a very promising synthetic route to introduce four or two 1,3-diketone-substituents to calix[4]arene via its upper rim, while its lower rim also provides an opportunity for modification. The 1,3-diketone calix[4]arenes have been already reported for their good antenna-effect on Tb³⁺-centered luminescence,¹⁷⁻¹⁹ although the property opens a new window for further improvement.

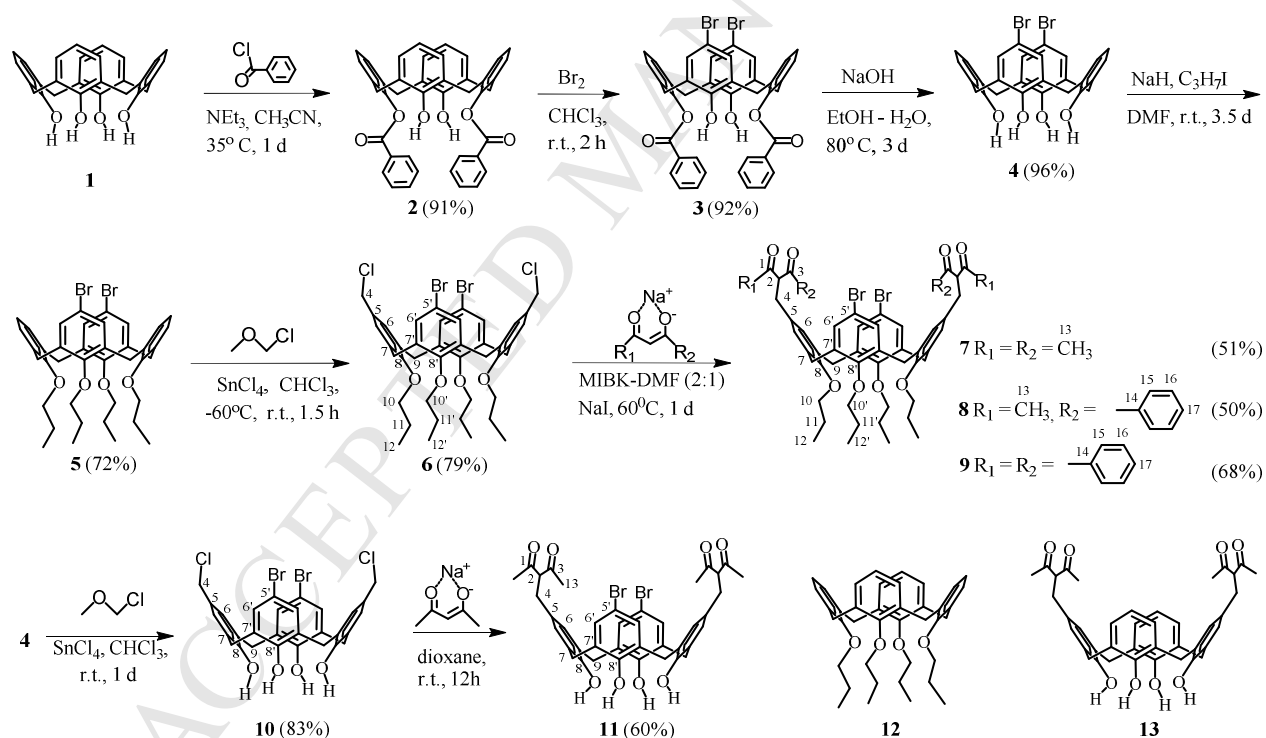
The antenna effect of a ligand is greatly affected by an efficacy of intersystem crossing. The introduction of halogen atoms into molecules can induce a strong spin-orbit coupling, which facilitates the intersystem crossing, well known as a heavy-atom effect.²⁰⁻²⁴ Thus, the dibromo-substitution of 2-carboxamide-8-hydroxyquinoline enhances significantly its antenna-effect on near-IR lanthanide-centered luminescence in the complexes with Nd³⁺, Er³⁺, Yb³⁺.²⁵

The present work suggests a versatile synthetic strategy for preparing novel calix[4]arene derivatives with a distal location of 1,3-diketone groups and "heavy" bromine atoms at the upper rim. The synthesized calix[4]arene derivatives contain hydroxy or propyloxy groups at the lower rim of the macrocyclic platform. All new compounds were characterized by different techniques such as IR, NMR, elemental analyses, UV-Vis, MALDI mass spectrometry and X-ray analysis. The complex formation and photoluminescent properties of ligands and their Tb³⁺ and Gd³⁺ complexes are reported. Additional information on the geometry of Tb³⁺ complexes was obtained from quantum-chemical calculations using Sparkle/PM7. The influence of structural peculiarity of calix[4]arenes on spectral properties of ligands and their lanthanide complexes is also discussed.

2. Results and Discussion

2.1. Synthesis and characterization of bis-1,3-diketone calix[4]arenes

The synthetic pathways for the bis-1,3-diketones are presented in Scheme 1. Selective upper rim dibromo-substitution of calix[4]arenes has been achieved by using dibromo derivative **4** as a key intermediate which was obtained by a sequential transformation of tetrahydroxycalix[4]arene **1** into **2**, **3** and **4** applying the protection and deprotection procedures as it was described elsewhere.²⁶ At the first synthetic stage, the distal substituted dibenzoyl product **2** was prepared. The bromination of **2** has been accomplished by using a slightly modified procedure where only 8 molar equivalents of Br₂ instead of 20 have been applied, with the reaction time being increased up to 2 hours. The reaction was quenched by vigorous stirring with saturated solution of sodium thiosulfate. The deprotection procedure was accomplished in basicified boiling water-ethanol solution and resulted in dibromo derivative **4**.



Scheme 1. Synthetic routes and structural formulae of the investigated compounds **1-13**. The similar numbering system of atoms for the compounds is used in the Table 1.

Compound **4** was successfully applied as a key reagent both in the synthesis of bis-1,3-diketones (**7-9**) having alkyl substituents at the low rim and for preparing unsubstituted analogue **11**. The tetra-alkyl derivative **5** has been synthesized by the interaction of calix[4]arene **4** with an excess of *n*-propyl iodide. The halogen methylation of **4** and **5** in the presence of an excess of

chloromethyl methyl ether and tin tetrachloride lead to the corresponding dichloromethyl derivatives **10** and **6** with good yields. The synthesis of bis-1,3-diketone derivatives **7-9** was fulfilled similarly to the synthesis of 3-substituted derivatives of pentane-2,4-dione.²⁷⁻²⁸ Addition of a sodium salt of the corresponding 1,3-diketone to the 5,17-bis-(chloromethyl)-25,26,27,28-tetrapropylcalix[4]arene **6** in the mixture of methyl isobutyl ketone (MIBK) and DMF in the presence of NaI under heating at 60 °C brought about the desired products **7-9**. The synthesis of bis-1,3-diketone derivative **11** has been performed at the room temperature using 1,4-dioxane as solvent. A possibility to carry out the reaction in the mild conditions can be explained by the transformation of bis-chloromethyl derivative **4** into the intermediate product having a quinone structure and possessing enhanced reaction ability in solution.^{18,19} Despite the difference in reaction behavior, the target calix[4]arenes were isolated in both cases with good yields (50%-68% for **7-9** and 60% for **11**). The obtained compounds were characterized by the combination of NMR, IR and MS techniques. The 3D-structure of **9** was finally established by a single crystal X-ray crystallography.

IR-data are in accordance with the structures suggested for new bis-1,3-diketones. Thus, rather intense doublet absorption bands $\nu(\text{C}=\text{O})$ are observed in the spectra of these compounds (Fig. S12-S15). The vibration frequencies of these bands become lower when phenyl substituents are introduced in the molecule. The introduction of the alkyl substituents at the lower calix[4]arene rim resulted in the disappearance of the intense absorptions $\nu(\text{OH})$ under going from bis-1,3-diketone **11** to **7-9**. More broadened absorption bands at $\sim 1600 \text{ cm}^{-1}$ in the IR spectra of the compounds **7** and **11** in comparison with **8** and **9** are probably caused by the numerous spatial forms induced by the keto-enol tautomerism.

Assignment of signals in the NMR spectra (Fig. S6-S11 in ESI) was accomplished by means of 2D COSY, ^1H , ^{13}C HSQC and ^1H , ^{13}C HMBC experiments (Table 1). According to ^1H NMR data, CDCl_3 solutions of the compounds **7** and **11** contain $\sim 35\%$ and $\sim 30\%$ ($C_L = 30 \text{ mM}$) of the enol form, correspondingly. A similar content of the enol form ($\sim 39\%$) is observed for **13**¹⁹ which is the non-substituted structural counterpart of **11**. Thus, dibromo-substitution results in an insignificant effect on the keto-enol equilibrium. However, the replacement of methyl substituents for the phenyl ones leads to a decrease of the amount of enol form under 8% for **8** and makes it practically undetectable for **9**. Bis-1,3-diketone **7** bearing alkyl substituents at the lower rim is characterized by narrow and more resolved signals in the ^1H NMR spectrum in comparison with its unsubstituted analogue **11**. This allowed us to establish the content of the three main forms for the compound **7** in CDCl_3 solution: ketone-ketone - 50%, ketone-enol - 30% and enol-enol - 20%.

Table 1. ^1H and ^{13}C chemical shifts^a (ppm) and spin-spin coupling constants (Hz) observed for calix[4]arenes **6-11** in CDCl_3 .

atom	compound											
	6		7^{b,c}		8		9		10		11^b	
	^1H	^{13}C	^1H	^{13}C	^1H	^{13}C	^1H	^{13}C	^1H	^{13}C	^1H	^{13}C
1			(16.84 (OH))	204.2 (192.1)	(17.12 (OH))	203.9		195.7			(16.85 (OH))	203.5 (192.2)
2			4.07	70.5 (109.2)	4.78	65.3	5.46 t, $^3J=6.5$	59.9			3.91 t, $^3J=7.3$	70.4 (108.1)
3						195.8						
4	4.33	45.8	3.09 k; 3.10 e (3.61 k, 3.58 e)	34.4 (32.8; 32.7)	3.21	34.6	3.32 d, $^3J=6.5$	34.9	4.47	45.8	3.01 d, $^3J=7.3$	33.4 (32.1) (3.50)
5		131.4		132.0 (131.9)		132.2		133.1		131.9		132.5 (135.0)
5'				115.2		115.2		115.2		114.4		114.3
6	6.66	128.9	6.86 k; 6.84 e (6.80 k; 6.79 e)	129.6 129.5 (128.7, 128.2)	6.82	129.7	6.82	129.5	7.11	129.9	6.87 (6.82)	129.6 (128.0)
6'	6.81		6.35 k, 6.34 e (6.37 e)	130.4 k, 130.3 e (130.5 e)	6.41	130.5	6.37	130.5	7.20	131.9	7.15	131.8
7		134.9		136.5 (136.2)		136.0		135.8		130.1		130.4 (130.2)
7'				135.8		135.9		135.8		128.0		130.2
8		156.9		156.3 κ 156.2 e (156.0 κ ; 155.9 e)		156.1		156.2	10.03 (OH)	149.1	9.98 (OH)	147.8 (147.4)
8'		155.8		154.6		154.9		154.8	10.03 (OH)	148.2	9.98 (OH)	148.0
9	3.12 <i>eq</i> d, $^2J=13.4$ 4.40 <i>ax</i> d, $^2J=13.4$	31.0	3.07 <i>eq</i> d, $^2J=13.3$ 4.36 <i>ax</i> d, $^2J=13.3$	31.0	3.05 <i>eq</i> s, br 4.34 <i>ax</i> s, br	31.3	3.02 <i>eq</i> d, $^2J=13.3$ 4.29 <i>ax</i> d, $^2J=13.3$	31.0	3.52 <i>eq</i> s, br 4.22 <i>ax</i> s, br	31.1	3.45 <i>eq</i> s, br 4.18 <i>ax</i> s,br	31.6
10	3.84 m	77.0	3.94	76.8	3.89	76.8	3.85 d, $^3J=6.9$	76.7				
10'			3.67	77.5	3.68	77.3	3.65 d, $^3J=6.9$	77.3				
11	1.90 m	23.3, 23.4	1.88	23.5	1.87	23.1	1.85 m	23.0				
11'			1.94	23.1	1.87	23.5	1.83 m	23.5				
12	0.99 t, $^3J=7.4$	10.4	0.89	10.0	0.89	10.1	0.90 t, $^3J=7.4$	10.0				
12'			1.07	10.8	1.05	10.8	1.04 t, $^3J=7.4$	10.8				
13			2.18 (2.13)	30.7 (23.6)	2.16	29.5					2.15 (2.05)	29.9 (23.4)
14						136.8		136.4				
15					7.96 d, $^3J=7.9$	129.0	7.93 d, $^3J=7.7$	128.8				
16					7.48 t, $^3J=7.9$	128.9	7.44 t, $^3J=7.7$	129.0				
17					7.58 t, $^3J=7.9$	133.7	7.54 t, $^3J=7.4$	133.7				

^a Numbering according to Scheme 1^b The assignment for the enol form of bis-1,3-diketone is given in parentheses^c Indexes k and e indicate the keto and enol forms of neighboring 1,3-diketone substituents

Similar to the parent compounds **6** and **10**, the new bis-1,3-diketones **7-9**, **11** have only a single peak of methylene-bridged carbon atoms in their spectra. According to the “de Mendoza rule”,²⁹ the determined values of chemical shifts ($\delta^{13}\text{C}(9) = 31.0\text{-}31.6$ ppm) indicate a *cone* isomer form for all investigated calix[4]arenes. Evidently, the observed picture is a result of a spatial averaging for three conformations: “boat 1”- “cone” – “boat 2”. An introduction of the substituents into the calix[4]arene platform substantially affects the inter-conversion process of the spatial forms, which is evident from the difference in chemical shifts ($\Delta^1\text{H}(9)$) between the axial and equatorial methylene protons of ArCH_2Ar groups.³⁰ The value of $\Delta^1\text{H}(9)$ for the propyl substituted calix[4]arenes **6-9** is 1.27-1.29 ppm and for tetrahydroxycalix[4]arenes **10** and **11** it is 0.7-0.73 ppm.

The colorless crystals of bis-1,3-diketone **9** suitable for X-ray analysis were obtained by the recrystallization of their crude products from $\text{MeOH-CH}_2\text{Cl}_2$. Compound **9** crystallizes in monoclinic $P2_1/c$ space group without inclusion solvate molecules in the crystal (Fig. 1). The calix[4]arene molecule is located in a special position in the crystal, notably on the two-fold rotational axis, therefore only one half of the molecule forms the symmetry independent part of the unit cell. The dihedral angles between the aromatic moieties and the plane defined by four carbon atoms of methylene bridges were determined as 84.4° and 139.8° , which indicates the “flattened cone” (“boat”) conformation of the molecule in crystal. In this conformation two opposite phenolic rings with 1,3-diketone substituents are turned out from the cavity and two Br-phenolic rings have an almost perpendicular orientation relative to the main plane of the macrocycle. The propyl groups are disordered over two positions with relative occupancy ratios of 0.58:0.42 and 0.69:0.31, respectively. It is worth noting that one pair of the propyl substituents is directed along the axial axis and the another is located in the equatorial plane of the calix[4]arene macrocycle. Both 1,3-diketone fragments of the molecule in the crystal exist in the keto form like in the solution of CDCl_3 and turn out from the cavity.

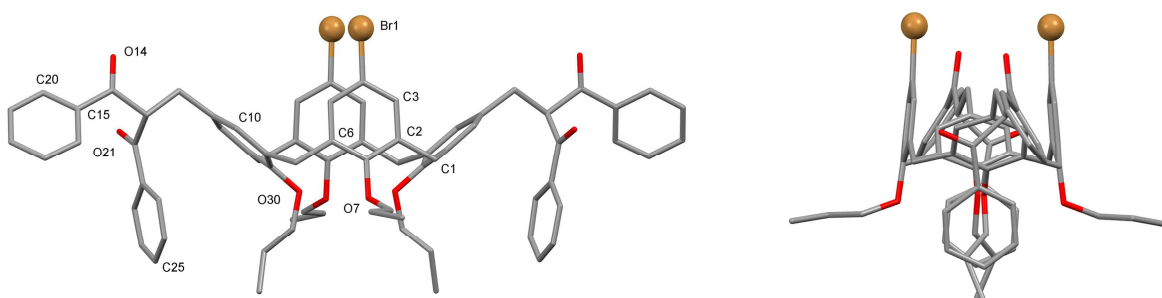


Fig. 1. Two projections of the molecule **9** with partial numbering scheme. Hydrogen atoms are omitted for clarity. All disordered propyl fragments are shown at the positions with greater occupancies.

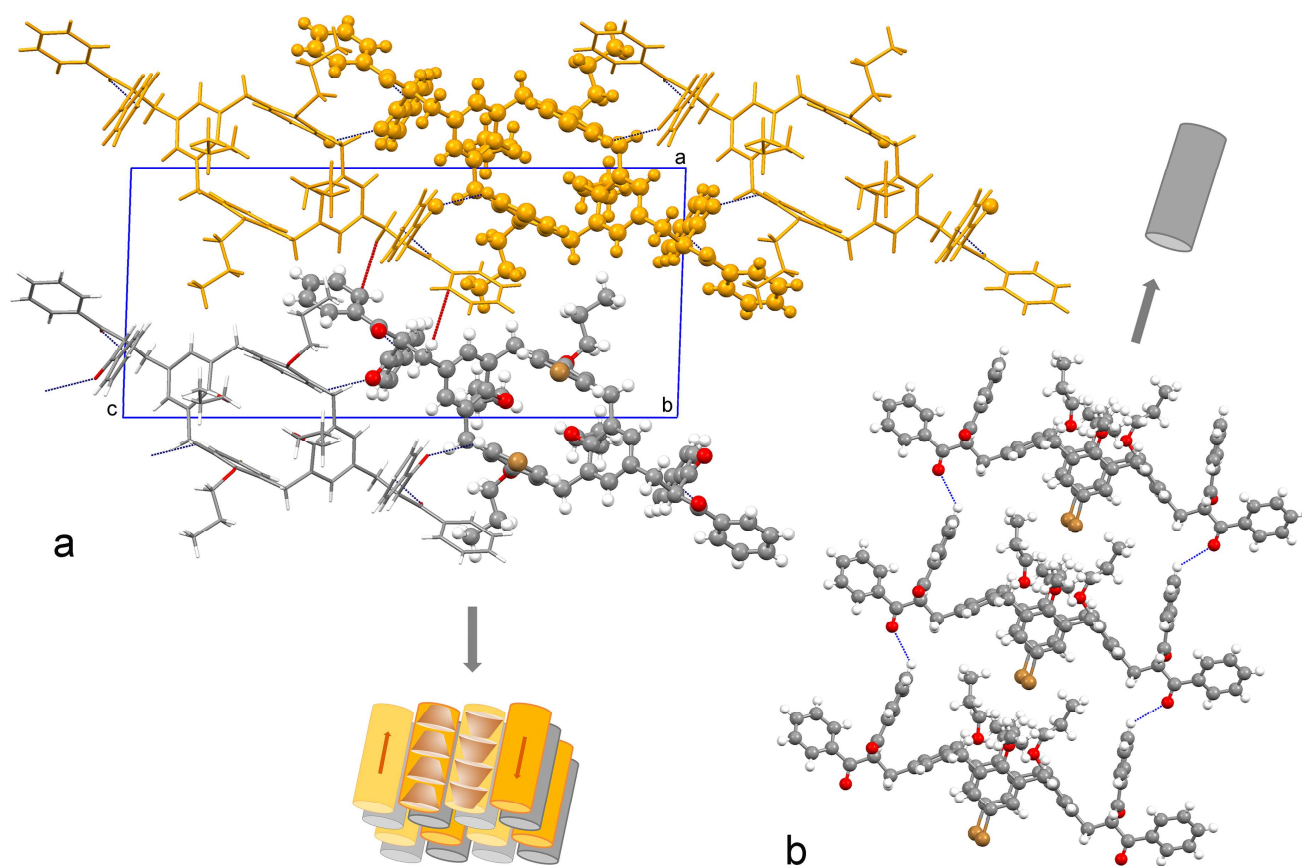


Fig. 2. Mutual arrangement of supramolecular layers (one of them is shown in orange color) in the crystal of **9**. C-H...O (blue color) and C-H... π (red color) interactions are shown by dashed lines (a). Fragment of C-H...O bonded (blue dashed lines) column in the crystal of **9** (b). Calix[4]arene molecules with the front and back orientations of macrocyclic cavity are shown in the “ball-stick” and “stick” model styles.

Table 2. Parameters of the intermolecular H-bonds and C-H... π contacts in the crystal of **9**.

D-H...A	H...A, Å	D...A, Å	\angle DHA, °	Symmetry operation
C25-H25...O14'	2.61	3.319(8)	134	x,-1+y,z
C3-H3...O21''	2.69	3.434(4)	138	x,1-y,1/2+z
C-H ...Cg ^a	H..Cg, Å	C-H..Cg, Å	C..Cg, Å	
(C10-H10)... (C15-C20)*	2.89	158	3.769(4)	1-x,1-y,-z
(C20-H20)... (C2-C7)**	2.99	117	3.509(4)	x,1-y,-1/2+z

^aCg – aromatic ring centroid.

The absence of donor groups capable of forming classical hydrogen bonds in the molecule

leads to another type of the structure-forming interactions in the crystal of **9** such as C-H...O and CH- π contacts, their parameters are presented in Table 2. It should be noted that all observed hydrogen bonds are paired due to the symmetry of molecule in crystal. A presence of paired hydrogen bonds C-H...O realized between the calix[4]arene molecules (C25-H25...O14) connected by a simple translation along the crystallographic axis 0b results in the formation of the H-bonded stack columns of the molecules arranged along the unit cell crystallographic axis 0b (Fig. 2). The integration of these columns is realized by means of paired hydrogen bonds C-H...O between the oxygen of the carbonyl group O21 and the hydrogen H3 belonged to the phenol fragment of the calix[4]arene framework. Additionally, the C-H... π contacts between H20 of the phenyl substituent and the π -system of the phenol fragment (C2-C7) of the calix[4]arene contribute to the process as well. The combination of these interactions leads to the formation of 2D-supramolecular layers arranged along 0bc plane in the crystal with an opposite location of the stack structures (the front or back oriented macrocyclic cavity). The layers are interconnected by means of the C-H... π interactions H10... Cg(C15-C20) (Table 2).

2.2. Electronic absorption spectroscopy

Both wavelength and efficacy of an electronic absorption are the most important criteria for the application of an organic ligand as a sensitizer of Ln³⁺-centered luminescence. Moreover, coordination ability of the new ligands with Tb³⁺ and Gd³⁺ ions can be also monitored through UV absorption spectra. Thus, UV absorption spectral measurements were performed with the aim to highlight the impact of the bromo-substitution on the coordination ability and antenna properties of the new bis-1,3-diketones **7-9** and **11**. For this reason, the absorption spectra were compared with those of calix[4]arenes **1**, **4**, **5**, **12** and **13**. The comparative results are represented in Fig. 3 and Table 3.

A comparison of UV spectra of the calix[4]arenes **1** and **4** demonstrates that incorporation of two Br atoms at the upper rim of the macrocyclic platform leads to both bathochromic shift of the main absorption band derived from π - π^* transitions and the increased molar absorption coefficients ($\Delta\lambda_{\max} = 9$ nm and $\Delta\epsilon_{\max} = 0.51 \times 10^3$ M⁻¹cm⁻¹). An attachment of the alkyl substituents at the low rim of calix[4]arene is followed by an opposite effect. Thus, the molar absorption coefficients become lower by approximately $\sim 7-8 \times 10^3$ M⁻¹cm⁻¹ when going from **11** to **7** and from **4** to **5**. However, a bathochromic shift ($\Delta\lambda_{\max} \sim 4-5$ nm) in such cases is also observed. The difference in the spectral features of **7** and **11**, as well as **5** and **4** results from the contribution of phenolate groups to electronic absorption due to the deprotonation of the phenolic moieties, which are involved into the cyclic hydrogen bonding of the lower calix[4]arene rim.³¹ Moreover, literature data³² indicate that bromo-substitution should additionally enhance the deprotonation of the phenolic groups.

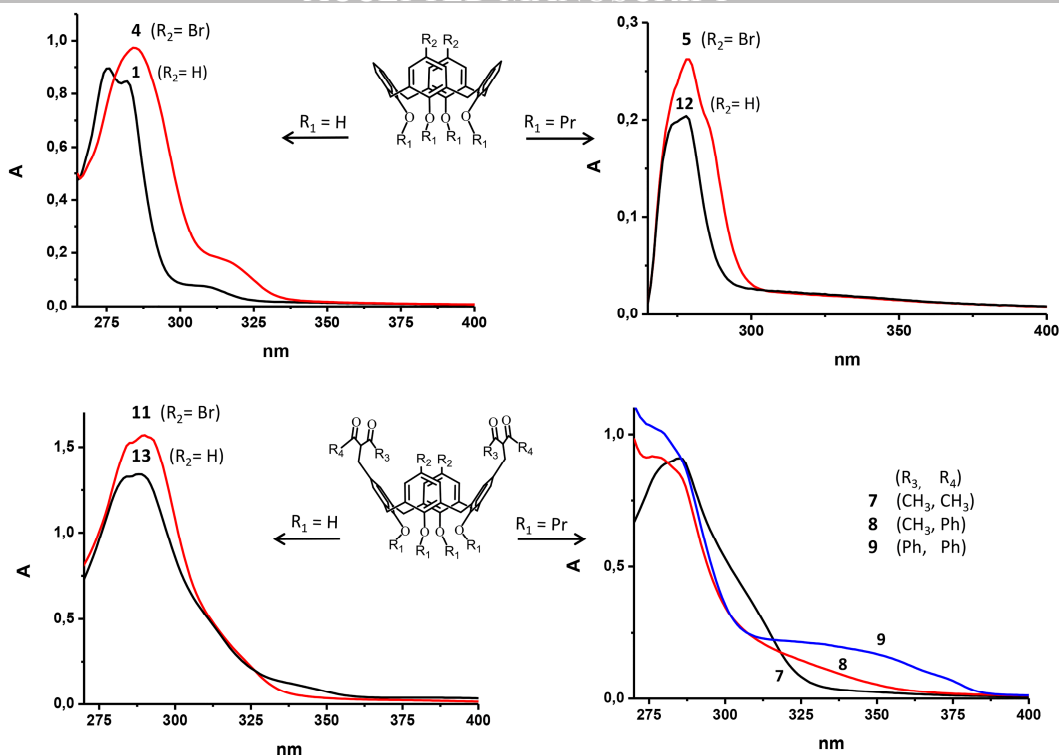


Figure 3. UV spectra for compounds **1**, **4**, **5**, **7-9**, and **11-13** in DMF ($C = 0.1$ mM).

Table 3. UV spectral data for compounds **1**, **4**, **5**, **7-9** and **11-13** in DMF.

Compound	λ_{\max} (nm)	ϵ_{\max} (10^3 M $^{-1}$ cm $^{-1}$)	Compound	λ_{\max} (nm)	ϵ_{\max} (10^3 M $^{-1}$ cm $^{-1}$)
1	275; 282	9.22; 8.83	9	280	9.98
4	284	9.73	11	289	15.71
5	279	2.62	12	278	2.04
7	285	7.72	13	288	13.42
8	280	9.06			

UV spectral patterns for 1,3-diketone derivatives are complicated by the additional absorption of ketone and enol forms. The shoulders at ~ 310 - 320 nm in the spectra of **7** and **11** can be attributed to the singlet-singlet $^1\pi$ - π enolic transitions in the 1,3-diketone moieties. The substitution of methyl groups by the phenyl ones in these fragments appeared as a broad absorption band in the range of 310-360 nm for **8** and as rather intense peak at 310-380 nm for **9**.

UV absorption spectra provide a sensitive tool to monitor the complex formation of 1,3-diketones with lanthanides, which was successfully used in evaluation of the complex formation in our previous reports.¹⁷⁻¹⁹ According to NMR data, the investigated bis-1,3-diketones are preferably in the ketone form. An addition of triethylamine (TEA) to the DMF solutions of the ligands did not lead to any changes in their spectra (Fig. S1a-c in ESI), while the changes observed for 25,26,27,28-

tetrahydroxycalix[4]arene **11** result from the contribution of phenolate-groups (Fig. S1d). Addition of Tb^{3+} ions to the basified DMF solutions of the ligands **7**, **8** and **9** results in the enhanced electronic absorption at 308 nm, 325 nm and 347 nm, respectively (Fig. S1 a-c). Similar changes were observed on the addition of Gd^{3+} ions (Fig. S1 a-c). The more pronounced changes for ligand **11** arise from the contribution of the deprotonated phenolic rim, although the predominant coordination of the lanthanide ions occurs via 1,3-diketonate groups due to the greater thermodynamic stability of the coordination via two 1,3-diketonates versus phenolate groups.¹⁹

The stoichiometry of Tb^{3+} complexes with bis-1,3-diketones **7**, **8** and **11** in DMF solutions has been estimated by using a Job plot analysis (Fig. 4). The maxima on the Job plots (Fig.4a,c) are not sharp, but they clearly point to the predominance of 1:1 complex formation for ligands **7** and **11**. It is worth noting that time-dependent complex formation for the compound **8** and especially for **9** was observed. In the latter case, however, the equilibrium has not been achieved even after 3 days of solution storage. In particular, the complexes with 2:1 (L: Tb^{3+}) stoichiometry are accumulated in the initial solutions in the case of **8**, followed by the time dependent transformation into more thermodynamically stable 1:1 complexes. Nevertheless, the Job plot shows greater deviations from the 1:1 binding for **8** than for **7** and **11** (Fig. 4). It is also worth noting that the storage of the initial solutions for 3 days improves the Job plots towards the 1:1 binding for all studied ligands. Thus, no reasonable data can be obtained in case of **9** because of too slow complex formation. The same effect of bulky α - and β -substituents on the keto-enol transformation of 1,3-diketone calix[4]arene derivatives in alkaline conditions was previously reported as the reason for the observed tendency.^{17,19}

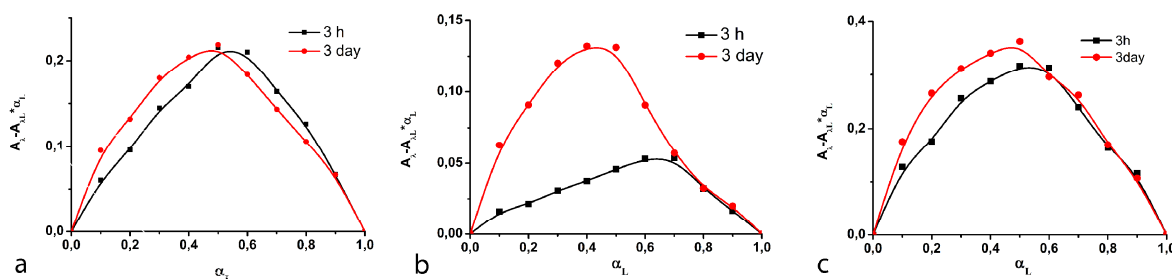


Figure 4. The Job plot profiles of DMF solutions at the varied time of solution storage (3h and 3 days) and L: Tb^{3+} molar ratios: (a) $\lambda = 310$ nm, $[Tb^{3+}] + [7] = 0.1$ mM, L:TEA (1:4); (b) $\lambda = 330$ nm, $[Tb^{3+}] + [8] = 0.1$ mM, L:TEA (1:4); (c) $\lambda = 320$ nm, $[Tb^{3+}] + [11] = 0.1$ mM, L:TEA (1:6). $\alpha_L = [L]/([L]+[Tb^{3+}])$.

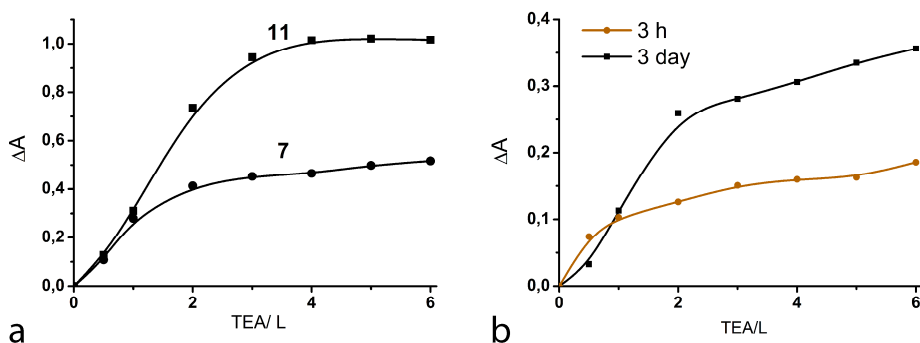


Figure 5. ΔA of the DMF solutions of **7** ($\lambda = 310$ nm), **11** ($\lambda = 320$ nm) (a) and **8** ($\lambda = 325$ nm) (b) with $\text{Tb}(\text{NO}_3)_3$ ($[\mathbf{7}] = [\mathbf{8}] = [\mathbf{11}] = [\text{Tb}^{3+}] = 0.1\text{mM}$) at varied TEA:L molar ratios and time of solutions storage 3 h (a), 3 h and 3 days (b).

The spectroscopic titration experiments were performed for ligands **7** and **11** at 1:1 (Tb: L) molar ratio with varying TEA:L molar ratio with the aim of evaluating the number of deprotonated groups in their Tb^{3+} complexes. The results are plotted as ΔA ($\Delta A = A - A_0$, where A and A_0 are the absorbances in basicified and in neutral solutions correspondingly) vs TEA:L molar ratio in Fig. 5. The results (Fig. 5a) confirm the participation of the both 1,3-diketonate groups of **7** in complex formation with Tb^{3+} . The deprotonation of a third proton for the compound **11** in its Tb^{3+} complexes arises from the lower phenolic rim.

A time resolved titration reveals the elimination of one proton only in the initial solution of ligand **8** within 3 hours (Fig. 5b), while the deprotonation of both 1,3-diketone groups requires 3 days of solution storage. This provides one more confirmation of the slow keto-enol transformation as the reason for the kinetically retarded complex formation.

2.3. The quantum-chemical calculation of structures of ligand **11** and its Tb^{3+} complexes

The obtained NMR and X-Ray data reveal the predominance of the *cone* isomer for new bis-1,3-diketones **7-9** and **11** both in the crystal state and in solution. The presence of bulky propyl substituents at the lower rim of the calix[4]arenes **7-9** prevents the conformational inversion of the molecule. In the case of the compound **11**, the situation is more complicated. The cyclic hydrogen bonding at the lower phenolic rim is the proposed reason for favoring the *cone* conformation.^{31]} However, the step-wise deprotonation of the phenolic groups in alkaline conditions can promote conformation shift from *cone* to the *partial cone* or 1,3-*alternate*. It is worth noting that the UV spectral titration experiments for **11** indicate such a probability. Nevertheless, the presence of bulky bromine atoms neighbouring to 1,3-diketonate groups can act as a factor influencing the conformation flexibility of **11**.

The geometry of ligand **11** and its complexes with Tb^{3+} can be revealed from quantum-chemical

calculations using the MOPAC 2012. Relative heat of formation for the conformers of calix[4]arene **11** and its complexes $[\text{Tb}^{3+}\text{L}^n]$ after semiempirical SPARKLE/PM7 optimization are presented in Table 4 and Figure 6. The obtained data show that the *cone* conformation is the most stable form for the ligand, and the *1,3-alternate* is the least efficient one. In the case of $[\text{Tb}^{3+}\text{L}^{2-}]$ complexes with two deprotonated 1,3-diketone groups, a similar order of the complex stability is observed: *cone* > *partial cone* > *1,3-alternate*.

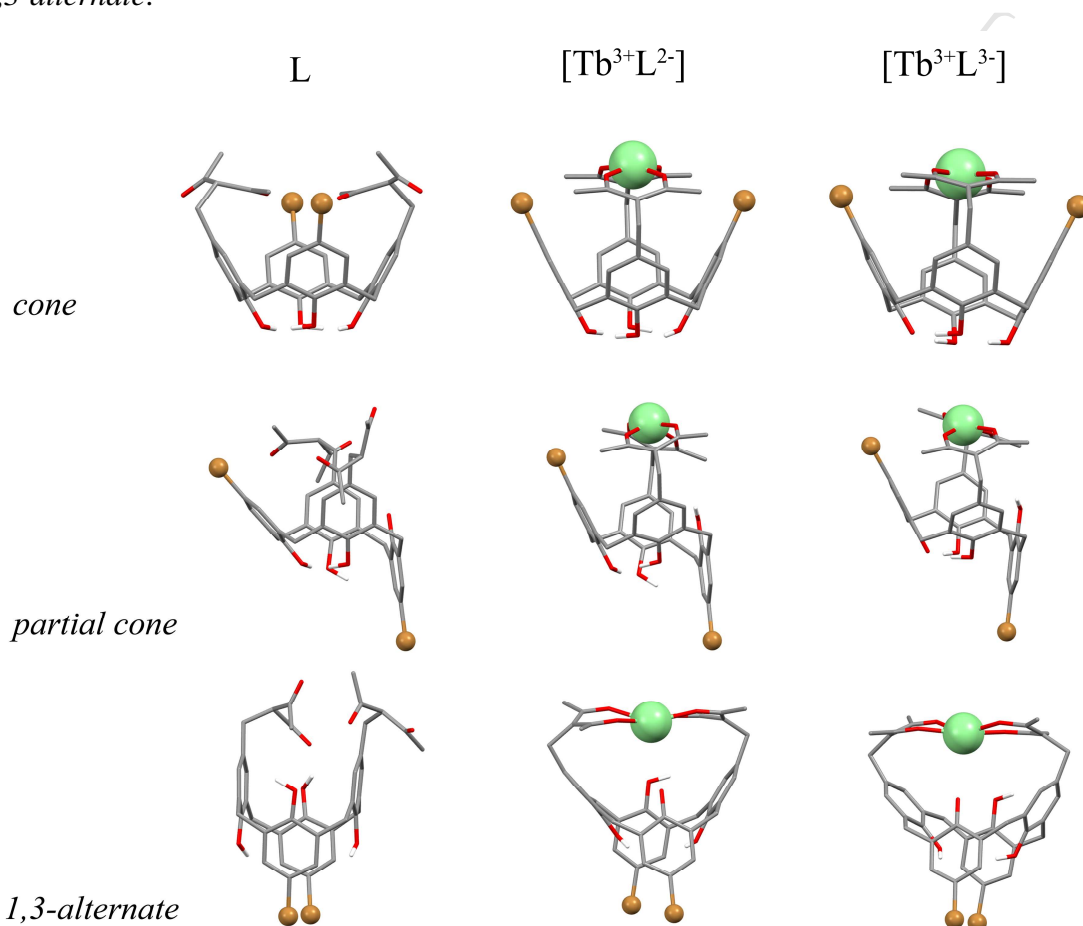


Figure 6. Sparkle/PM7 model optimized structures of three conformers of **11** and their Tb^{3+} complexes. Hydrogen atoms are omitted for clarity with the exception of the phenolic hydrogens.

Table 4. Relative heat of formations calculated for conformers of calix[4]arene **11** and its complexes $[\text{Tb}^{3+}\text{L}^n]$.

compound	ΔH_{298}° (kcal/mol)		
	<i>cone</i>	<i>partial cone</i>	<i>1,3-alternate</i>
L	0	21.08	24.87
$[\text{Tb}^{3+}\text{L}^{2-}]$	0	15.97	33.25
$[\text{Tb}^{3+}\text{L}^{3-}]$	0	16.33	34.87

The comparison of the quantum-chemical calculation data obtained for **11** and its analogue **13** without bromine atoms at the upper rim¹⁹ demonstrates that the dibromo-substitution favors the complexes with the ligand in the *cone* conformation against the complexes, where the ligand is in *partial cone* and *1,3-alternate* conformations by ~2.6 kcal/mol and ~5.9 kcal/mol, respectively.

Thus, the bromine atoms attached at the upper rim of bis-1,3-diketone calix[4]arene **11** result in the additional stabilization of the calix[4]arene backbone in *cone* conformation under the coordination of Tb³⁺ ion via two 1,3-diketonate groups of the ligand.

2.4. Photoluminescence spectroscopy

A comparative analysis of the photophysical properties of the lanthanide complexes with ligands **7**, **11** and **13** is required to reveal the impact of bromo-substitution on the antenna effect of the new ligands. Since, a sensitizing ability of any ligand is greatly guided by an efficacy of intersystem crossing, the photophysical properties of Gd³⁺ complexes with ligands **7**, **8**, **11** and **13** were measured. The main aim of the measurements is to detect the effect of both the upper and lower rim substituents on the ability of the ligands to sensitize Tb³⁺-centered luminescence.

Having no electronic energy levels below 32000 cm⁻¹, Gd³⁺ cannot accept any energy from triplet states of 1,3-diketonate ligands, but it induces the same optical shift and eventually enhances singlet-triplet transitions in 1,3-diketonate ligands by its heavy-atom effect.³³⁻³⁵ Nevertheless, emission of the Gd³⁺ complexes monitored at room temperatures can be contributed by both fluorescence and phosphorescence, while Gd³⁺ complexes become phosphorescent in frozen solution at low temperature. Thus, the recording of time-resolved luminescence spectra at both room and low temperatures is a widely applied route to discriminate singlet- and triplet-derived luminescence of Gd³⁺ complexes and to determine the energy of the lowest triplet state (T₁) of the ligands.

For the Gd³⁺ complexes with acetylacetonate-substituted ligands **7**, **11** and **13** the emission bands in the spectral range of 350-412 nm could be associated to fluorescence from excited singlet states of the ligands, since the decay time value of the bands is less than 3 μs at both 143 K and room temperatures. In contrast, the emission bands in the spectral range of 412-650 nm have temperature-dependent lifetime and therefore were attributed to the phosphorescence from the excited triplet states of the ligands (Figs S2, a, c, d in ESI). Similarly, for Gd³⁺ complex with acetylacetonate-substituted ligand **8** the emission bands in the 350-430 nm and 430-730 nm regions were associated with fluorescence and phosphorescence, correspondingly (Figure S2, b in ESI).

The luminescence of the Gd³⁺ complexes with the ligands **7** and **8** at room temperature and 143 K is contributed by both fluorescence and phosphorescence. The time-resolved luminescence spectra of these complexes show that intensities of the fluorescence bands decrease very fast as the time delay

is increased, while the intensity of the phosphorescence bands increases and only the phosphorescence from ligand is displayed at $T=143$ K and time delays of $100 \mu\text{s}$ (Figs. S2, a, b in ESI). It is worth noting that the luminescence spectra of the Gd^{3+} complexes with **11** and **13** are not contributed by the fluorescence in the lower temperature conditions at both 1 and $100 \mu\text{s}$ delay time (Figs. S2, c, d in ESI), that indicates a high rate of intersystem crossing for the complex. These results show that the lower rim substitution on going from **11** to **7** is the reason for the restricted intersystem crossing.

The excited state lifetime (τ) values for the luminescence of Gd^{3+} complexes with ligands **7**, **8**, **11** and **13** were evaluated from the luminescence decay curves at 143 K on the basis of three-exponential expansion. The equations for the calculation of the averaged τ -values are represented in detail in ESI. The phosphorescence of the Gd^{3+} complexes with **7**, **11** and **13** at 143 K is characterized by the three-exponential decay with the average lifetime values being $785 \mu\text{s}$, $927 \mu\text{s}$ and $738 \mu\text{s}$, correspondingly (Figure S3, Table S1 in ESI). On the contrary, the phosphorescence of the Gd^{3+} complex with **8** is characterized by the two-exponential decay with the average lifetime values being $1023 \mu\text{s}$. The comparison of the average lifetime values for the complexes with **11** and **13** reveals the effect of dibromo-substitution on the decay time of the triplet state of the ligands.

Figure 7 compares the phosphorescence spectra of Gd^{3+} complexes with ligands **7**, **8**, **11** and **13** at 143 K. The phosphorescence spectra of the complexes are characterized by the broad bands with maxima at 460 nm (21739 cm^{-1}), 506 nm (19763 cm^{-1}), 468 nm (21367 cm^{-1}) and 470 nm (21277 cm^{-1}), respectively. The T_1 state energy of the ligands can be determined from the phosphorescence peak at the shortest wavelength corresponding to a 0-0 phonon transition.³³ Since vibration structure of the phosphorescence spectra is not enough resolved, the decomposition of the spectra into Gaussian components was done for an accurate evaluation of the 0-0 phonon transition maxima (Figures S4 in ESI illustrate the decomposition of the spectra into Gaussian components). In particular, the 0-0 transition for Gd^{3+} complexes with ligands **7**, **8**, **11** and **13** are 430 nm (23250 cm^{-1}), 470 nm (21270 cm^{-1}), 438 nm (22830 cm^{-1}) and 441 nm (22670 cm^{-1}), correspondingly.

The analysis of the luminescence spectra of the Gd^{3+} complexes reveals the insignificant effect of the dibromo-substitution on the values of the T_1 states energies. Thus, the energy rise $\Delta T_1 \sim 160 \text{ cm}^{-1}$ is observed under going from **13** to **11**. The T_1 state energy of alkyl substituted ligand **7** is also increased ($\sim 420 \text{ cm}^{-1}$) in compare with the unsubstituted analogue **11**. This tendency indicates that the T_1 state energy of the new bis-1,3-diketonates is somewhat affected by the lower rim substituents. The significant red shift ($\sim 40 \text{ nm}$, $\Delta T_1 = 1980 \text{ cm}^{-1}$) on going from acetylacetone ligand **7** to the benzoylacetone one **8** is in good agreement with our previous report,¹⁹ where the benzoylacetone-substituted counterpart of **13** was revealed as a convenient antenna for the near-IR luminescence of the Yb(III) complex.

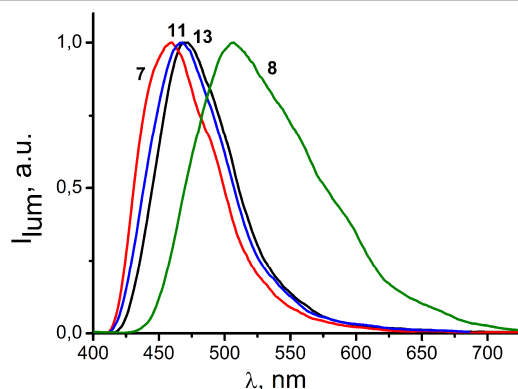


Figure 7. Normalized phosphorescence spectra of the Gd^{3+} complexes with ligands **7**, **8**, **11** and **13** at 100 μs time delay and $T = 143\text{ K}$.

Summarizing the optical spectroscopy data it is worth noting that the T_1 state energy is notably affected by the phenyl-substitution of 1,3-diketonate moieties ($\Delta T_1 = 1980\text{ cm}^{-1}$), while the lower rim substitution and dibromo-substitution results in very small if any effect on this value ($\Delta T_1 \sim 160\text{-}420\text{ cm}^{-1}$). The average lifetime values are significantly enhanced by dibromo-substitution, although they are decreased by the lower rim substitution (Table S1). The revealed tendencies are of great impact in the antenna properties of the ligands, which was exemplified by the Tb^{3+} -centered luminescence of the corresponding complexes with ligands **7** and **11**, excluding the complex with **8**, where the T_1 state energy of the ligand (21270 cm^{-1}) is too low to feed the excited state of Tb^{3+} .

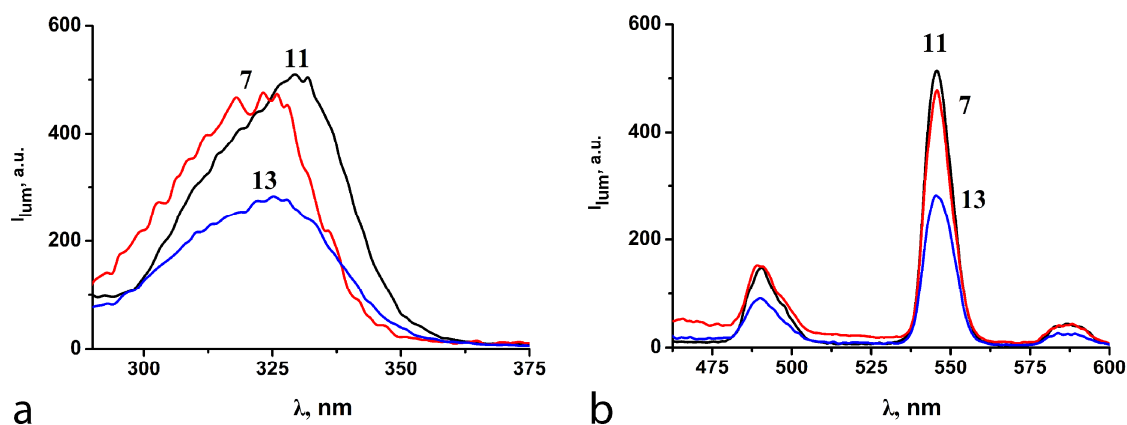


Figure 8. Excitation (a) and luminescence spectra (b) of basicified DMF solutions of Tb^{3+} with ligands **7** ($\lambda_{\text{ex}}=326\text{ nm}$), **11** ($\lambda_{\text{ex}}=330\text{ nm}$) and **13** ($\lambda_{\text{ex}}=325\text{ nm}$) within one day after the sample preparation. $C_{\text{L}} = C_{\text{Tb}^{3+}} = 0.1\text{ mM}$, $C_{\text{TEA}} = 0.4\text{ mM}$.

The Tb^{3+} -centered luminescence spectra of the Tb^{3+} complexes with ligands **7**, **11** and **13** presented in Figure 8 confirm the structural impact on the antenna effects of the ligands. Moreover, the increased steady state luminescence intensities (~ 1.7) for Tb^{3+} complexes with dibromo derivatives **11** and **7** versus the similar value for **13** correlate with the lifetime values, which are 0.20 and 0.22 ms for

11 and **7** correspondingly. These values are greater than the $\tau = 0.12$ ms previously reported for the Tb^{3+} complexes with **13**.¹⁹ The decay curves for the Tb^{3+} -centered luminescence are presented in Fig. S5.

3. Conclusions

In summary, we have synthesized novel upper-rim dibromo-substituted bis-acetylacetonate derivatives of calix[4]arenes with hydroxy and propyloxy groups at the lower rim. Additionally, the bis-benzoylacetonate and -dibenzoylmethane derivatives of 25,26,27,28-tetrapropoxy-calix[4]arene were also obtained. The NMR, X-Ray data and quantum chemical calculations indicate that all synthesized calix[4]arenes adopt a *cone* conformation.

The obtained results highlight the effects of different substituents on the keto-enol and conformational transformations, which are of great importance on the complex formation with lanthanide ions. In particular, the dibromo-substitution of an upper rim of bis-acetylacetonate calix[4]arene derivatives stabilizes the *cone* conformation without any detectable retardation of the keto-enol transformation. The dibromo-substitution does not influence the retardation of the keto-enol transformation when acetylacetonate is substituted by benzoylacetonate. Thus, dibromo-substituted bis-acetylacetonate calix[4]arene derivatives are revealed as most convenient ligands for Gd(III) and Tb(III) ions, where the coordination of lanthanide ions via two acetylacetonate moieties is facilitated by the stabilized *cone* conformation.

The analysis of low temperature optical spectroscopy data of Gd(III) complexes with the differently substituted calix[4]arene derivatives reveals that the energy of the triplet state is significantly affected by the substitution of the acetylacetonate to benzoylacetonate groups. The time-resolved measurements of the complexes demonstrate a significant heavy-atom effect on the triplet state lifetime of the ligands. In particular, an increase in averaged lifetime values is observed on going from bis-acetylacetonate calix[4]arene to its dibromo-substituted analogue, while these values are somewhat decreased by lower rim substitution.

The measurements of Tb^{3+} -centered luminescence indicate the improvement of an antenna-effect of bis-acetylacetonate calix[4]arene derivatives by dibromo-substitution. The increased steady state luminescence intensities (~ 1.7) for Tb^{3+} complexes with the dibromo-substituted derivatives correlate with the excited state lifetime values, which is in good confirmation with the heavy-atom effect on the decay of the triplet state of the dibromo-substituted ligands.

The obtained results should contribute to further design of organic ligands for the development of new luminescent materials.

4. Experimental Section

4.1. Materials

Acetylacetone was distilled before use. Methyl isobutyl ketone (MIBK) (Acros Organics) and *N,N*-dimethylformamide (DMF) (Acros Organics) was distilled over P₂O₅. CDCl₃ (99.8% isotopic purity) from Aldrich was used for NMR spectroscopy. 1-Benzoylacetone, dibenzoylmethane, triethylamine (Acros Organics) and terbium nitrate (Tb(NO₃)₃•xH₂O) (Alfa Aesar) were used as commercially received without further purification.

Synthesis: The synthetic routes, the structural formulae and numbering of atoms of the investigated compounds are shown in Scheme 1. The calix[4]arenes **1**,³⁶ **2-4**²⁶ and sodium salts of acetylacetone (NaAA), 1-benzoylacetone (NaBA), dibenzoylmethane (NaDBM)¹⁹ were obtained as described in literature. ¹H and ¹³C chemical shifts and spin-spin coupling constants observed for new synthesized calix[4]arenes **6-11** are presented in Table 1.

4.2. Synthesis of 5,17-dibromo-25,26,27,28-tetra(1-propyloxy)calix[4]arene **5**

5,17-Dibromo-25,26,27,28-tetrahydroxycalix[4]arene **4** (1.75 g, 3 mmol) and 1-iodopropane (2.9 ml, 30 mmol) were added to a suspension of NaH (0.96 g, 60%, 24 mmol) in DMF (50 ml), previously washed with *n*-hexane. After stirring for 3.5 days under argon at ambient temperature, the reaction mixture was quenched with 2 *N* HCl (40 ml). The resulting precipitate was washed sequentially with water and methanol. The solid was boiled in MeOH under stirring for 0.5 h. Then the colorless product was dried at 90 °C in vacuo to give 1.63 g (2.16 mmol, 72%) of the calix[4]arene **5**. Mp. 247-252 °C. Anal. calcd for C₄₀H₄₆Br₂O₄ (750.60): C, 64.01; H, 6.18, Br, 21.29. Found: C, 64.48; H, 6.35; Br, 21.03. The spectroscopic parameters of the product **5** are the same as those obtained for this compound synthesized in another way.^{37,38}

4.3. Synthesis of 5,17-dibromo-11,23-bis-(chloromethyl)-25,26,27,28-tetra(1-propyloxy)-calix[4]arene **6**

Chloromethyl methyl ether (136 mmol, 21 ml (6.53 M/l)) was added to the calix[4]arene **5** (2.55 g, 3.4 mmol) in a dry chloroform (50 mL) under argon atmosphere. The solution was cooled to -60 °C, and tin tetrachloride (2.4 ml, 20 mmol) was added dropwise under vigorous stirring. Stirring was continued for 0.5 h and then the mixture was allowed to reach room temperature. Then after keeping a reaction mixture in such conditions for 1 h, the cold water (30 ml) was added. The solution was vigorously stirred until bleaching has been achieved. The organic layer was separated, washed twice with water (30 ml, 10%), dried over MgSO₄ and concentrated by distillation. After trituration in

MeOH and evaporation of solvent at 65 °C in a high vacuo, the target calix[4]arene **6** was obtained as a white powder with a yield of 79% (2.29 g, 2.7 mmol). Mp. 198-203 °C. Anal. calcd for C₄₂H₄₈Br₂Cl₂O₄ (847.54): C, 59.52; H, 5.71. Found: C, 59.68; H, 5.47.

4.4. General procedure for the synthesis of bis-1,3-diketone ligands 7-9

NaI (0.269 g, 1.8 mmol) was added to the solution of calix[4]arene **6** (0.5 g, 0.6 mmol) in the mixture of MIBK (10 ml) and DMF (5 mL) under argon atmosphere. Mixture was stirring at 35 °C for ~ 0.5 h until a complete salt dissolving has been observed. After addition of a sodium salt of 1,3-diketone (1.8 mmol, 0.223 g of NaAA, 0.331g of NaBA or 0.443 g of NaDBM), the stirring of solution was continued for 1 day at 60 °C. Then the solvent was removed from the reaction mixture by distillation at the reduced pressure. Dichloromethane (20 ml) and 2 M HCl (20 ml) were added to the residue at vigorous stirring. The organic layer was separated, sequentially washed with water, 10% Na₂S₂O₃ (15ml) and water again. The organic layer was then dried over MgSO₄ and concentrated by distillation. Solvent residues were removed at 90 °C *in vacuo*. After trituration of the remainder in MeOH and evaporation of the solvent at 90 °C, the target calix[4]arenes **7-9** were obtained.

4.4.1. *Synthesis of 5,17-dibromo-11,23-bis-[(acetylaceton-3-yl)methyl]-25,26,27,28-tetra(1-propyloxy)-calix[4]arene 7.* White powder, yield 51% (0.30 g, 0.31 mmol). Mp. 120-125 °C. IR (nujol, cm⁻¹): ν 3443 (vbr, ν(OH)), 1728, 1701 (ν(C=O)), 1603, 1574 (ν(C=O) and ν(C=C)), 1458 (ν(Ph)), 1378, 1356, 1306, 1253, 1224, 1199, 1169, 1154 (ν_{as}(CCC)), 1066, 1040, 1005, 963 (ν_s(CCC)). Anal. calcd for C₅₂H₆₂Br₂O₈ (974.85): C, 64.07; H, 6.41; Br, 16.39. Found: C, 64.26; H, 6.17; Br, 16.13. Mass spectrum (MALDI-TOF): m/z: = 995.2 [M+Na]⁺.

4.4.2. *Synthesis of 5,17-dibromo-11,23-bis-[(benzoylaceton-3-yl)methyl]-25,26,27,28-tetra(1-propyloxy)-calix[4]arene 8.* White powder, yield 50% (0.33 g, 0.30 mmol). Mp. 98-103 °C. IR (nujol, cm⁻¹): ν = 3437 (vbr, ν(OH)), 17180, 1678 (ν(C=O)), 1597, 1580 (ν(C=O) and ν(C=C)), 1458 (ν(Ph)), 1378, 1356, 1261, 1220, 1199 (ν_{as}(CCC)), 1067, 1039, 1004, 964 (ν_s(CCC)). Anal. calcd for C₆₂H₆₆Br₂O₈ (1098.99): C, 67.76; H, 6.05; Br, 14.54. Found: C, 67.46; H, 6.18; Br, 14.77. Mass spectrum (MALDI-TOF): m/z: = 1119.3 [M+Na]⁺.

4.4.3. *Synthesis of 5,17-dibromo-11,23-bis-[(dibenzoylmethan-3-yl)methyl]-25,26,27,28-tetra(1-propyloxy)-calix[4]arene 9.* White powder, yield 68% (0.50 g, 0.41 mmol). Mp. 115-120 °C. IR (nujol, cm⁻¹): ν = 3473 (vbr, ν(OH)), 1693, 1672 (ν(C=O)), 1597, 1581 (ν(C=O) and ν(C=C)), 1458, (ν(Ph)), 1377, 1338, 1268, 1227, 1197 (ν_{as}(CCC)), 1066, 1003, 963 (ν_s(CCC)). Anal. calcd for C₇₂H₇₀Br₂O₈

(1223.13): C, 70.70; H, 5.77; Br, 13.07. Found: C, 70.57; H, 5.98; Br, 13.29. Mass spectrum (MALDI-TOF): $m/z = 1243.2 [M+Na]^+$.

4.5. Synthesis of 5,17-dibromo-11,23-bis-(chloromethyl)-25,26,27,28-tetrahydroxy-calix[4]arene **10**

Chloromethyl methyl ether (20 mmol, 3 ml (6.53 M)) was added to a solution of 5,17-dibromo-25,26,27,28-tetrahydroxy-calix[4]arene **4** (0.29 g, 0.5 mmol) in dry chloroform (30 ml) under argon atmosphere at the room temperature. Tin tetrachloride (0.35 ml, 3 mmol) was added dropwise to the mixture under vigorous stirring. Stirring was continued for 1 day and then 1M HCl (30 ml) was added. The mixture was vigorously stirred until bleaching of the solution has been observed. The organic layer was separated, washed twice with dilute acetic acid (30 ml, 10%), dried over $MgSO_4$ and concentrated by distillation. Solvent residues were removed at 55 °C in high vacuo. The target calix[4]arene **10** was obtained with the yield 83% (0.28 g, 0.42 mmol). Mp. > 260 °C (decomp.). Anal. calcd for $C_{30}H_{24}Br_2Cl_2O_4$ (679.23): C, 53.05; H, 3.56. Found: C, 53.28; H, 3.35.

4.6. Synthesis of 5,17-dibromo-11,23-bis-[(acetylaceton-3-yl)methyl]-25,26,27,28-tetrahydroxy-calix[4]arene **11**

To a solution of 5,17-dibromo-11,23-bis-(chloromethyl)-25,26,27,28-tetrahydroxy-calix[4]arene **10** (0.203 g, 0.3 mmol) in anhydrous dioxane (100 ml) NaAA (0.112 g, 0.9 mmol) was added under stirring. Addition of Na salt to the reaction mixture was accompanied by a grey-violet coloring. After stirring the reaction mixture at room temperature for 12 h, the dioxane was distilled off under reduced pressure. The residue was acidified by 1 M HCl (50 ml) and diluted with CH_2Cl_2 (50 ml). The mixture was vigorously stirred until a clear solution formed. The organic layer was separated, washed several times with water, dried over $MgSO_4$ and concentrated by distillation. The crude product was boiled thoroughly in a small amount of MeOH, filtered off and washed by MeOH again. After evaporating of the rest of solvent at 80 °C in a high vacuo, the target calix[4]arene **11** as a white powder was obtained. Yield 60% (0.15 g, 0.18 mmol). Mp. > 185 °C (decomp.). IR (nujol, cm^{-1}): $\nu = 3171$ (vbr, $\nu(OH)$), 1726, 1698 ($\nu(C=O)$), 1603 ($\nu(C=O)$ and $\nu(C=C)$), 1459 ($\nu(Ph)$), 1377, 1260, 1209, 1166 ($\nu_{as}(CCC)$), 951 ($\nu_s(CCC)$). Anal. calcd for $C_{40}H_{38}Br_2O_8$ (806.53): C, 59.57; H, 4.75; Br, 19.81. Found: C, 59.32; H, 4.53; Br, 20.10. Mass spectrum (MALDI-TOF): $m/z = 827.2 [M+Na]^+$.

4.7. Methods

Microanalyses of C and H were carried out with a EuroVector CHNS-O Elemental Analyser EA3000. Melting points of compounds were measured with a Boetius hotstage apparatus. MALDI mass spectra were detected on a Bruker Ultraflex III MALDI-TOF/TOF mass spectrometer. NMR experiments were performed on a Bruker AVANCE-600 spectrometer at 303K equipped of a 5 mm diameter broadband probe head working at 600.13 MHz in ^1H and 150.864 MHz in ^{13}C experiments. Chemical shifts in ^1H and ^{13}C spectra were done relative to the solvent as internal standard (CDCl_3 $\delta(^1\text{H})$ 7.27 ppm, $\delta(^{13}\text{C})$ 77.2 ppm). Assignment of signals of NMR spectra was accomplished by means of 2D COSY, ^1H - ^{13}C HSQC and ^1H - ^{13}C HMBC experiments. The pulse programs of the COSY, HSQC and HMBC experiments were taken from Bruker software library. IR absorption spectra were recorded on a Vector-22 Bruker FT-IR spectrophotometer with a resolution of 4 cm^{-1} as Nujol emulsions and KBr pellets of compounds.

UV spectra have been recorded on a Lambda 35 spectrophotometer (Perkin-Elmer) in 10 mm quartz cuvettes. The Job plots and spectrometric titrations were done from monitoring absorbance (A_λ).

The steady-state and time-resolved Tb^{3+} centered luminescence spectra have been recorded on a spectrofluorometer FL3-221-NIR (Jobin Yvon) with SPEX FL-1042 phosphorimeter in 10 mm quartz cuvettes. Excitation of samples has been performed at the wavelength values designated in figure captions and emission detected at 545 nm for Tb^{3+} with 6/6 nm excitation and emission slits. Time-resolved measurements have been performed on a spectrofluorometer FL3-221-NIR (Jobin Yvon) using the following parameters: time per flash-49.00 ms, flash count-200 ms, initial delay-0.02 ms and sample window-2 ms. The measurements were performed at room temperature in aerated conditions.

The time-resolved luminescence spectra of the Gd^{3+} complexes were recorded using an optical spectrometer based on an MDR-23 grating monochromator (LOMO, Saint Petersburg, Russia) coupled to a FEU-100 photomultiplier tube.³⁹ The luminescence was excited by an LGI-21 pulsed nitrogen laser (337 nm wavelength, 2.1 mW laser pulse average output power, 10 ns pulse duration, 100 Hz repetition rate). The average output power of the laser near the samples was 1.7 mW. The exposed surface areas of the samples were 7 mm^2 . The measurements were performed at different temperatures in aerated conditions.

4.7.1. X-ray Crystallographic Details for Compound 9

The X-ray diffraction data for the crystal of **9** was collected on a Bruker Kappa Apex II CCD diffractometer in the ω and ϕ -scan modes using graphite monochromated $\text{Mo K}\alpha$ ($\lambda = 0.71073\text{ \AA}$) radiation at 296(2) K. Data were corrected for the absorption effect using SADABS program.⁴⁰ The structure was solved by direct method and refined by the full matrix least-squares using SHELXTL⁴¹ and WinGX⁴² programs. All non-hydrogen atoms were refined anisotropically. The hydrogen atoms

were inserted at calculated positions and refined using a riding models. Data collections: images were indexed, integrates and scaled using the APEX2⁴³ data reduction package. Analysis of the intermolecular interactions was performed using the program PLATON.⁴⁴ Mercury program package⁴⁵ was used for figures preparation.

Crystallographic data (excluding structure factors) for the structure **9** has been deposited in the Cambridge Crystallographic Data Centre as supplementary publication number CCDC 1544897. Copies of the data can be obtained free of charge upon application to CCDC, 12 Union Road, Cambridge CB2 1EZ, UK, (fax: 44(0)1223 336033 or e-mail: deposit@ccdc.cam.ac.uk).

Crystallographic data for **9**: C₇₂H₇₀O₈Br₂, colorless prism, size 0.49x0.35x0.21 mm³, $M = 1223.10$, monoclinic, $a = 11.785(2)$ Å, $b = 10.0515(19)$ Å, $c = 26.215(5)$ Å, $\beta = 91.954(3)^\circ$, $V = 3103.7(10)$ Å³, $T = 296(2)$ K, space group $P 2/c$, $Z = 2$, $\mu(\text{Mo K}\alpha) = 1.362$ mm⁻¹, $\rho_{\text{calc}} = 1.309$ g·cm⁻³, $F(000) = 1272$, theta range for data collection 2.026 to 28.921°, 58527 reflections measured, 7938 independent reflections ($R_{\text{int}} = 0.0949$), 393 parameters, 9 restraints. Final indices: $R_1 = 0.0567$, $wR_2 = 0.1428$ (3723 reflections with $I > 2\sigma_I$), $R_1 = 0.1384$ (all data), $wR_2 = 0.1814$ (all data), GoF = 1.001, largest difference in peak and hole (0.458 and -0.477 eÅ⁻³).

4.7.2. Quantum-chemical computations

Structural modeling of complexes was performed with the use of MOPAC 2012 software.⁴⁶ The PM7 semiempirical method was applied⁴⁶ with using of Sparkle/PM7 Lanthanide Parameters⁴⁷ for the Modeling of Tb³⁺ complexes which allowed to minimize computational time and resources and to maintain the accuracy comparable to non-empirical approaches.

Acknowledgements

This work was supported by the Russian Fund for basic Research (grant 16-03-00007 A).

Appendix A. Supplementary data

Supplementary data (IR, UV, ¹H and ¹³C NMR spectra, crystallographic data of compound **9**, luminescence spectra and decay curves of complexes, the determination of the T₁ state energy) related to this article can be found at <http://dx.doi.org/XXXXXXXXXXXX>.

References

1. Amoroso AJ, Pope SJA *Chem. Soc. Rev.* 2015;44:4723–4742.
2. Heffern MC, Matosziuk LM, Meade TJ *Chem. Rev.* 2014;114:4496–4539.
3. Bünzli J-CG *Coord. Chem. Rev.* 2015;293:19–47.
4. Kuriki K, Koike Y, Okamoto Y *Chem. Rev.* 2002;102:2347–2356.
5. Martins JP, Martín-Ramos P, Coya C, Alvarez AL, Pereira LC, Díaz R, Martín-Gil J, Silva MR *Mater. Chem. Phys.* 2014;147:1157–1164.
6. Yersin H *Highly Efficient OLEDs with Phosphorescent Materials*, Wiley, London 2008.
7. Reid BL, Stagni S, Malicka JM, Cocchi M, Sobolev AN, Skelton BW, Moore EG, Hanan GS, Ogden MI, Massi M *Chem. Eur. J.* 2015;21:18354–18363.
8. Binnemans K *Chem. Rev.* 2009;109:4283–4374.
9. An BL, Gong ML, Li M-X, Zhang J-M, Cheng Z-X *J. Fluoresc.* 2005;15:613–617.
10. Xi P, Gu XH, Chen CF, He YX, Huang XA *Spectrochimica Acta Part A* 2007;66:667–671.
11. Song XQ, Zheng JR, Liu WS, Ju ZH *Spectrochimica Acta Part A* 2008;69:49–55.
12. Carter KP, Thomas KE, Pope SJA, Holmberg RJ, Butcher RJ, Murugesu M, Cahill CL *Inorg. Chem.* 2016;55:6902–6915.
13. Park J, Lee JH, Jaworski J, Shinkai S, Jung JH *Inorg. Chem.* 2014;53:7181–7187.
14. Faulkner S, Matthews JL, Ward MD *Comprehensive Coordination Chemistry*, Elsevier, Oxford, UK 2004;9:913–941.
15. Moore EG, Samuel APS, Raymond KN *Acc. Chem. Res.* 2009;42:542–552.
16. Samuel APS, Xu J, Raymond KN *Inorg. Chem.* 2009;48:687–698.
17. Shamsutdinova NA, Podyachev SN, Sudakova SN, Mustafina AR, Zairov RR, Burilov VA, Nizameev IR, Rizvanov IK, Syakaev VV, Gabidullin BM, Katsuba SA, Gubaidullin AT, Safiullin GM, Dehaen W *New J. Chem.* 2014;38:4130–4140.
18. Zairov R, Shamsutdinova N, Podyachev S, Sudakova S, Gimazetdinova G, Rizvanov I, Syakaev V, Babaev V, Amirov R, Mustafina A *Tetrahedron* 2016;72:2447–2455.
19. Podyachev SN, Sudakova SN, Gimazetdinova GSh, Shamsutdinova NA, Syakaev VV, Barsukova TA, Iki N, Lapaev DV, Mustafina AR *New. J. Chem.* 2017;41:1526–1537.
20. McGlynn SP, Azumi T, Kinoshita M *Molecular Spectroscopy of the Triplet State*, Prentice Hall, Englewood Cliffs, N. J. 1969;7.
21. Sivchik VV, Solomatina AI, Chen Y-T, Karttunen AJ, Tunik SP, Chou P-T, Koshevoy IO *Angew. Chem. Int. Ed.* 2015;54:14057–14060.
22. He Y, Liu L, Zhang Z, Fu G, Lü X, Wong W-K, Jones RA *Inorg. Chem. Commun.* 2016;64:13–15.

23. Tong GSM, Chow PK, Che C-M *Angew. Chem. Int. Ed.* 2010;49:9206–9209.
24. Sun C-L, Li J, Geng H-W, Li H, Ai Y, Wang Q, Pan S-L, Zhang H-L *Chem. Asian J.* 2013, 8, 3091–3100.
25. Albrecht M, Osetska O, Klankermayer J, Fröhlich R, Gumyd F, Bünzli J-C G. *Chem. Commun.* 2007;1834–1836.
26. Schühle DT, Klimosch S, Schatz J *Tetrahedron Lett.* 2008;49:5800–5803.
27. Podyachev SN, Sudakova SN, Galiev AK, Mustafina AR, Syakaev VV, Shagidullin RR, Bauer I, Konovalov AI *Russ. Chem. Bull.* 2006;55:2000–2007.
28. Staniszewski B, Urbaniak W *Chemical Papers* 2009;63:212–216.
29. Jaime C, De Mendoza J, Prados P, Nieto PM, Sanchez C J. *Org. Chem.* 1991;56:3372–3376.
30. Bohmer V *Angew. Chem., Int. Ed. Engl.* 1995;34:13–745.
31. Lang J, Deckerová V, Czernek J, Lhoták P *J. Chem. Phys.* 2005;122:044506.
32. Serjeant EP, Dempsey B *Ionization Constants of Organic Acids in Aqueous Solution*, Pergamon, Oxford 1979.
33. Sager WF, Filipescu N, Serafin FA *J. Phys. Chem.* 1965;69:1092–1100.
34. Arakawa M, Tanaka I *J. Phys. Chem.* 1985;89:5649–5654.
35. Tobita S, Arakawa M, Tanaka I *J. Phys. Chem.* 1984;88:2697–2702.
36. Gutsche CD, Levine JA, Sujeeth PK *J. Org. Chem.* 1985;50:5802–5806.
37. Casnati A, Fochi M, Minari P, Pochini A, Riggiani M, Ungaro R, Reinhoudt DN *Gazz. Chim. Ital.* 1996;126:99–106.
38. Stastny V, Lhoták P, Stibor I, König B *Tetrahedron* 2006;62:5748–5755.
39. Lapaev DV, Nikiforov VG, Safiullin GM, Galyaviev IG, Dzabarov VI, Knyazev AA, Lobkov VS, Galyametdinov YuG *J. Struct. Chem.* 2009;50:775–781.
40. Sheldrick GM *SADABS*, Program for empirical X-ray absorption correction, *Bruker-Nonius* 2004.
41. Sheldrick GM *SHELXTL* v.6.12, Structure Determination Software Suite, *Bruker AXS*, Madison, Wisconsin, USA 2000.
42. Farrugia LJ *WinGX* 1.64.05. *J. Appl Cryst.* 1999;32:837.
43. *APEX2* (Version 2.1), *SAINTPlus*, Data Reduction and Correction Program (Version 7.31A), *BrukerAXS* Inc., Madison, Wisconsin, USA 2006.
44. Spek AL Single-crystal structure validation with the program *PLATON*, *J. Appl Cryst.* 2003;36:7.
45. Bruno IJ, Cole JC, Edgington PR, Kessler MK, Macrae CF, McCabe P, Pearson J, Taylor R *Acta Cryst.* 2002;58:389.
46. Stewart JJP *MOPAC* 2012.

47. Dutra JDL, Filho MAM, Rocha GB, Freire RO, Simas AM, Stewart JJP *J. Chem. Theory and Comput.* 2013;9:3333–3341.

ACCEPTED MANUSCRIPT

Captions for the illustrations:

Scheme 1. Synthetic routes and structural formulae of the investigated compounds **1 - 11**. The similar numbering system of atoms for the compounds is used in the Table 1.

Fig. 1. Two projections of the molecule **9** with partial numbering scheme. Hydrogen atoms are omitted for clarity. All disordered propyl fragments are shown at the positions with greater occupancies.

Fig. 2. Mutual arrangement of supramolecular layers (one of them is shown in orange color) in the crystal of **9**. C-H...O (blue color) and C-H... π (red color) interactions are shown by dashed lines (a). Fragment of C-H...O bonded (blue dashed lines) column in the crystal of **9** (b). Calix[4]arene molecules with the front and back orientations of macrocyclic cavity are shown in the “ball-stick” and “stick” model styles.

Figure 3. UV spectra for compounds **1, 4, 5, 7-9**, and **11-13** in DMF ($C = 0.1$ mM).

Figure 4. The Job plot profiles of DMF solutions at the varied time of solution storage (3h and 3 days) and L:Tb³⁺ molar ratios: (a) $\lambda = 310$ nm, [Tb³⁺] + [**7**] = 0.1 mM, L:TEA (1:4); (b) $\lambda = 330$ nm, [Tb³⁺] + [**8**] = 0.1 mM, L:TEA (1:4); (c) $\lambda = 320$ nm, [Tb³⁺] + [**11**] = 0.1 mM, L:TEA (1:6). $\alpha_L = [L]/([L]+[Tb^{3+}])$.

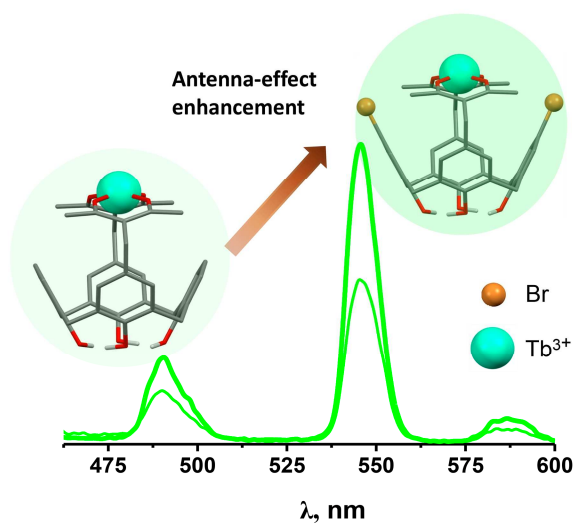
Figure 5. ΔA of the DMF solutions of **7** ($\lambda = 310$ nm), **11** ($\lambda = 320$ nm) (a) and **8** ($\lambda = 325$ nm) (b) with Tb(NO₃)₃ ([**7**] = [**8**] = [**11**] = [Tb³⁺] = 0.1mM) at varied TEA:L molar ratios and time of solutions storage 3 h (a), 3 h and 3 days (b).

Figure 6. Sparkle/PM7 model optimized structures of three conformers of **11** and their Tb³⁺ complexes. Hydrogen atoms are omitted for clarity with the exception of the phenolic hydrogens.

Figure 7. Normalized phosphorescence spectra of the Gd³⁺ complexes with ligands **7, 8, 11** and **13** at 100 μ s time delay and T = 143 K.

Figure 8. Excitation (a) and luminescence spectra (b) of basicified DMF solutions of Tb³⁺ with ligands **7** ($\lambda_{ex}=326$ nm), **11** ($\lambda_{ex}=330$ nm) and **13** ($\lambda_{ex}=325$ nm) within one day after the sample preparation. $C_L = C_{Tb^{3+}} = 0.1$ mM, $C_{TEA} = 0.4$ mM.

Graphical Abstract



New *bis*-1,3-diketone calix[4]arene derivatives adopting *cone* conformation with dibromo-substituted upper rim of calix[4]arene backbone are introduced as ligands for lanthanide ions with improved sensitization of Tb³⁺-centered luminescence due to heavy-atom effect.

New bis-1,3-diketone calix[4]arene derivatives adopting cone conformation with dibromo-substituted upper rim of calix[4]arene backbone are introduced as ligands for lanthanide ions with improved sensitization of Tb³⁺-centered luminescence due to heavy-atom effect.

ACCEPTED MANUSCRIPT